

Layer-by-Layer Assembled Oxidative Films as General Platform for Electrodeless Formation of Conducting Polymers

Mikko Salomäki,^{*,†,‡} Ossi Myllymäki,[†] Minna Hätönen,[†] Juho Savolainen,[†] and Jukka Lukkari^{†,‡}

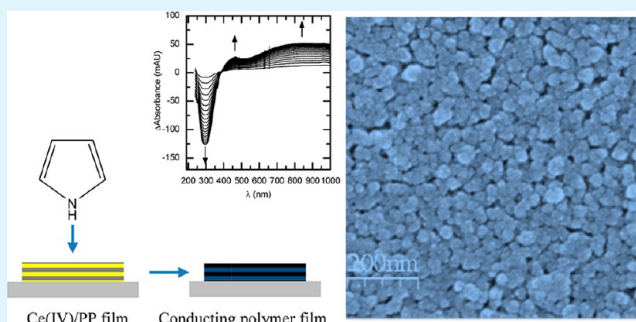
[†]Department of Chemistry, University of Turku, FI-20014 Turku, Finland

[‡]Turku Centre for Materials and Surfaces (MatSurf), FI-20014 Turku, Finland

S Supporting Information

ABSTRACT: Fabrication of precisely tailored layers of conductive polymers in thin film assemblies is an attractive extension of the layer-by-layer technique. This approach provides tools for fabricating thin films with customized optical and electrical properties. In this paper, we study inorganic layer-by-layer assembled films prepared using polyphosphate and cerium(IV). It is shown that these multilayers can oxidize certain monomers from the adjacent aqueous solution to produce conducting polymer layers. We studied the thermodynamic factors that allow the aforementioned autopolymerization. A five bilayer polyphosphate/cerium(IV) film was shown to possess high oxidative power in acidic solutions. It was found that the polymerization of pyrrole, aniline and 3,4-ethylenedioxythiophene in contact with the redox active multilayer is thermodynamically favored. The rate of polymer formation and the thickness of the conducting film could be controlled by the concentration of the monomer in solution and the number of cerium/polyphosphate bilayers in the oxidative film. The oxidative polymerization of pyrrole was unambiguously recognized on UV-vis spectra with characteristic reduction and oxidation bands. The film formation was not restricted by charge diffusion and the reaction formally followed first-order kinetics. The results suggest that the reaction takes place effectively within the whole pre-existing polypyrrole film and it continues until all oxidant in the film was used. The spectral changes that are characteristic for conducting polypyrrole are shown on spectroelectrochemical analysis of the films indicating that cationic (polaron) and dicationic (bipolaron) species are involved in the redox processes of the film. The functional polymer films formed are found to be electroactive and conducting. Therefore, they fully resemble of conducting polymer films prepared using traditional electropolymerization.

KEYWORDS: layer-by-layer, oxidative film, polyphosphate, cerium, conducting polymers, polypyrrole



INTRODUCTION

The sequential layer-by-layer (LbL) self-assembly of oppositely charged components is a general technique for a controlled and reproducible preparation of various types of thin films. The assembly proceeds via alternating adsorption of polyanions and polycations and is essentially insensitive to the size, shape, and material of the substrate. This technique offers the possibility to create thin films with an almost unlimited variety of components and does not require high-level experimental set-up or strictly controlled conditions.¹ The manipulation of conjugated polymers is a potential extension of the layer-by-layer technique. It provides tools for fabricating thin films containing customized optical and electrical properties. Thin films of conducting polymers offer possibilities for new applications in, e.g., electrostatic materials, molecular electronics, displays, chemical, biochemical and thermal sensors, drug release systems, electromagnetic shielding, etc.² Many of these applications include a sufficiently thin film of conducting polymer that is prepared on substrates of different size, shape and chemical nature. The fabrication of films with thickness control at the molecular level sets high requirements for the

preparation method of the film. The LbL assembly offers means for manipulating conjugated polymers at the nano level. Traditionally, the incorporation of conducting polymers in the LbL films has been done using either p-type-doped conducting polymers³ or conducting polyelectrolytes, i.e., conducting polymers that have pendant charged groups in their repeat units.^{4,5} Also, conducting polymer-ionomer mixtures, such as poly(3,4-ethylenedioxythiophene):poly(styrene sulfonate) (PEDOT:PSS), have been used in the LbL studies.⁶ All the aforementioned methods have their advantages but there are also limitations in the controllability of the build-up process or the electrical quality of the films.

In our previous paper, we showed that functional, purely inorganic LbL films can be prepared using polyphosphate (PP) as the polyanion and a tetravalent metal ion, cerium(IV), as the cationic component, and that these multilayers can oxidize pyrrole monomers from the adjacent aqueous solution to

Received: October 3, 2013

Accepted: January 23, 2014

Published: January 23, 2014

produce thin conducting polymer layers.⁷ Cerium(IV) is known as very versatile one electron oxidant.⁸ Some of the recognized advantages of cerium(IV) are its high reduction potential and low toxicity. It can oxidatively polymerize conducting polymers from their monomer solutions.^{9,10} Cerium(IV) is also capable of polymerizing vinyl monomers, such as acrylamide or acrylonitriles with the free radicals, which occurs by a redox reaction between Ce(IV) and a reducing agent.^{11–13} On the other hand, conducting polymers have been prepared on cerium containing template materials using various procedures. Conducting polymer nanocomposites have been prepared on self-supported sheets of fibrous Ce(IV) hydrogen phosphate.¹⁴ Modification of montmorillonite particles with Ce(IV) results in functional particles that can polymerize pyrrole or 3,4-ethylenedioxythiophene (EDOT) from the adjacent solution.^{15,16} In addition, cerium(IV) oxide particles have been shown to polymerize pyrrole on their surface and thus form conducting polymer composite materials.¹⁷ On a solid surface, an applied cerium(IV) oxide coating can also act as an oxidative surface for polypyrrole formation.^{18,19} These reported Ce(IV) template-based oxidative polymerization methods, however, have limitations in the nature, size, and form of the substrate materials. In addition, there are several reports on, e.g., polypyrrole formation on particles and porous or polymeric substrates by treating the substrate with oxidant and exposing it to monomers (or vice versa).²⁰ In this case, the conductivity generally depends on the pyrrole loading in the resulting material, high loading, and thick films resulting in well-conducting materials.

Polypyrrole (PPy) is one of the most important conducting polymers because of its high electrical conductivity, high stability, redox reversibility and ease of synthesis. On the other hand, there are limitations for the extensive use of PPy because of its relative fragility structure and insolubility. In general, certain requirements have to be satisfied for the surface generated oxidation of monomer molecules from the adjacent solution. The effective redox potential of the film in contact with the solution must be higher than the oxidation potential of the monomer and the amount of the oxidizing species in the film must be sufficiently high to maintain the oxidation reaction long enough in order to deposit a layer of conducting polymer. The mechanism of the oxidative polymerization of various monomers by a chemical oxidant is principally similar to the electropolymerization of conjugated polymers. The mechanism, with some marginal adjustments, is widely accepted in the literature.²¹ Generally, in the polymerization process the monomers are oxidized to radical cations, which then dimerize, in case of pyrrole and thiophenes at the α -position. This is followed by elimination of two protons from the doubly charged dimer, resulting in a neutral aromatic dimer. This dimer, because of its greater conjugation, is more easily oxidized than the monomer and, upon oxidation, it undergoes the next coupling step with a monomeric radical cation, resulting in charged trimer. Polymerization proceeds via a cascade of chain propagation reaction.

In this paper, we extend our previous study of oxidative Ce/PP multilayers to the considerations of the basic thermodynamic and kinetic factors that control the success of the electrodeless conducting polymer film formation on these multilayers. In addition, we demonstrate the generality of the system by showing that the same oxidative multilayer is capable of polymerizing 3,4-ethylenedioxythiophene (EDOT) and aniline from aqueous solutions, too. The resulting polymers,

poly(3,4-ethylenedioxythiophene), or PEDOT, and polyaniline, are among the most studied and useful conducting polymers because of their high electrical conductivity, strong electrochromism, and high stability in ambient conditions. The thin films have been electrochemically characterized before and after the conducting polymer film formation and the thermodynamic requirements of the polymerization reaction are clarified. The kinetics of the Ce/PP-multilayer catalyzed oxidation and polymerization reactions have been followed by UV–vis spectroscopy and the redox properties of the polymer films characterized using spectroelectrochemical measurements. The electrical properties and the morphology of the polymer films have been studied by conductivity measurements and atomic force microscopy (AFM) and scanning electron microscopy (SEM). Special attention has been devoted to the polymer film formation mechanism and the factors affecting it.

■ EXPERIMENTAL SECTION

Preparation of coating solutions was made by following procedure: 10 mM (referring to monomer concentrations) of potassium polyphosphate (potassium metaphosphate, ABCR) was solubilized in aqueous solution of 0.1 M NaCl. The solution was stirred for approximately 18 h and then filtered with a 0.45 μ m filter. Cerium(IV) ammonium nitrate (Merck), zirconium(IV) oxychloride octahydrate was solubilized in water as 10 mM solutions. The pH of metal ion solutions was unadjusted and was approximately 1.5. Pyrrole (Acros Organics), 3,4-ethylenedioxythiophene (EDOT, Bayer), and aniline (Merck) were used as received.

Multilayer films were deposited in following manner: At each deposition step the coating solution was allowed to stay in contact with the substrate exactly for 15 min followed by rinsing with water for three times. These steps were repeated alternately with anionic and cationic coating solutions until data for the wanted number of layers were achieved.

For cyclic voltammetry and redox potential measurements a miniature gold electrode was electrochemically cleaned by cycling in 0.5M H₂SO₄ until the voltammogram of pure gold was achieved. Then it was primed with a monolayer of 2-mercaptoethylamine (Aldrich) by immersing the electrode to 1 mM water solution for an hour. A multilayer film was deposited on a gold electrode and the electrode was placed in an electrolyte solution together with a sodium-saturated SCE reference electrode (SSCE) and the potential difference between the electrodes was monitored under open-circuit conditions. Keithley multimeter 2000 was used in the open-circuit potential measurements. Autolab PGSTAT101 potentiostat was used in cyclic voltammetry measurements.

For the UV-vis spectroscopy a quartz flow-through cuvette was cleaned inside with piranha solution (3:1 concentrated sulfuric acid to 30% hydrogen peroxide solution), rinsed with water, and dried. Then it was silanized with 1% solution of N-(trimethoxysilylpropyl)-N,N,N-triethylammonium chloride (ABCR) in methanol for 30 minutes, in order to obtain a positively charged surface. All the measurements concerning kinetics of the film formation were carried out at 25 °C.

Spectroelectrochemical experiments were performed in a cuvette using film-covered ITO glass slide as a working electrode and a conventional three-electrode cell. The multilayer film was deposited on ITO glass slide treated similarly as in the case of quartz cuvette. The reference electrode was miniature Ag/AgCl electrode and platinum wire was the auxiliary electrode. All the potentials are referred to the SSCE electrode.

For QCM measurements the quartz crystal (10 MHz, 100 nm gold plating with a chromium adhesion layer, Lap-Tech, Inc., South Bowmanville, Ontario) was primed with a monolayer of 2-mercaptoethylamine and coated with polyphosphate and cerium(IV) ions in a fully automated system. The prototype QCM is the same as in our previous papers.^{22,23} At each step the coating solution was allowed to stay in contact with the crystal exactly for 15 min and after rinsing with the supporting electrolyte the QCM measurement was

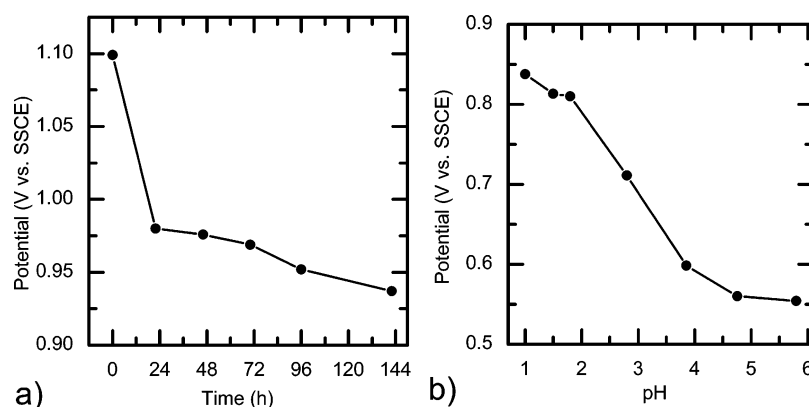


Figure 1. Effective oxidation potential of PP/Ce multilayer films vs. the SSCE reference electrode. (a) Potential of a five-bilayer film vs. age of the film measured in 0.1M Na₂SO₄, pH 1.5. The film stored in air in between the measurements. (b) Potential of a five-bilayer film as a function of solution pH in a 0.1M Na₂SO₄ (pH adjusted with H₂SO₄).

done. These steps were repeated alternately with anionic and cationic coating solutions until data for the wanted number of layers were collected. Coating and measurements were done at 25 °C.

Electrical conductivity of the samples was measured using van der Pauw four-point probe method using Keithley 2400 source meter. The electrical contacts to the sample were done with four mercury capillaries arranged in a form of square with side length of 5 mm.

The morphology of the films was studied by scanning electron microscopy, SEM (LEO Gemini 1530). The atomic force microscopy images were recorded on a diCaliber AFM microscope (diCaliber, Bruker) operated in the tapping mode.

RESULTS AND DISCUSSION

Thermodynamic Considerations. Thermodynamics sets the limits for the oxidative power of the films. The oxidative driving force of the Ce/PP multilayer is given by the effective redox potential of the Ce(IV)/Ce(III) pair in the film. In order to estimate the redox potential and to study its dependence on experimental conditions for optimal behavior we have measured the open-circuit potential of an electrode covered with a Ce/PP multilayer. We have previously found, based on the X-ray photoelectron spectroscopy (XPS) results, that an aged film (vide infra) contains approximately equal amounts of Ce(IV) and Ce(III), which implies that the effective standard potential of the redox pair may be approximated by the measured open-circuit potential of an aged multilayer.⁷ In pristine films, the Ce(IV)/Ce(III) ratio and, consequently, the effective oxidation power of the film are given by the measured potential.

The study of the redox behavior of the multilayer is complicated by the time dependence of the open-circuit potential (Figure 1a). The film was measured in acidic (pH 1.5) electrolyte solution (0.1 M Na₂SO₄) and it was kept dry between measurements. At pH 1.5, a freshly prepared (PP/Ce)₅ film has a redox potential close to 1.1 V. Initially, the decrease in potential takes place very rapidly, but the rate stabilizes to ca 10 mV/day after the initial drop. The initial fast potential drop signifies a change in the Ce(IV)/Ce(III) ratio by ca. two orders of magnitude and, if we use the final potential value from Figure 1a as a rough estimate of the effective standard potential at this pH we can estimate that this initial rapid decrease corresponds to the increase of the Ce(III) fraction in the multilayer from practically zero to ca. 0.4%. Actually, this is an overestimate because the film has not reached the equimolar state during the time span of Figure 1a (see, for example, the starting value of Figure 1b). Therefore,

this initial drop can be attributed to the reaction of a small amount of oxidizable species in the solution and in air with Ce(IV) in the film. On the other hand, during multilayer preparation, each immersion into a Ce(IV) solution drives the cerium in the film to the higher oxidation level, re-establishing the pristine oxidation state. Finally, in time, the aged film reaches a maximally redox buffered state, in which it contains an approximately equimolar amount of Ce(IV) and Ce(III), as discussed in our earlier work.⁷ However, the results show that the prepared multilayers possess a high and relatively stable (in the time scale of several hours or even days) oxidative power.

Various other factors affect the redox potential of the Ce(IV)/Ce(III) pair, too, the pH of the solution being one of the most important. The redox potential of this redox pair is well established in acidic water solutions and it decreases with pH.^{24,25} This can be attributed to the preferential complexation of Ce(IV) by OH⁻ ions already in neutral and in relatively acidic aqueous solutions, which starts already at the proton concentration of [H⁺] = 0.2 M.^{26,27} The open-circuit potential of the (PP/Ce)₅ multilayer in a 0.1 M Na₂SO₄ solution as a function of solution pH is shown in Figure 1b. Above pH 2 the potential decreases rather linearly until it levels up at ca pH 4-5 and the linear part follows an equation $E^{\circ}(\text{Ce}^{4+}/\text{Ce}^{3+}) = 1.00 \text{ V} - 0.11 \text{ V pH}$ (vs. SSCE), suggesting a (2H⁺, 1e⁻) redox process. Comparison with published values of the effective standard potentials shows that the cerium species involved in the redox reaction cannot be unambiguously identified, which is understandable considering the complex chemical environment within the multilayer.²⁷ Although our previous XPS work indicated the presence of CeO₂ in dry films, that was most probably an artifact caused by the drying process.⁷ However, the qualitatively similar behavior of the redox potential of the Ce species bound inside the film and those in solution shows that the multilayer structure does not hamper the redox properties of cerium(IV). Therefore, the film functions as an active oxidative matrix, despite the cerium-polyphosphate and other unspecified complexes involved, and its oxidative power increases with decreasing pH. In addition, even at neutral pH, the multilayer exhibits relatively high oxidation potential.

In addition to time and pH, the thickness of the multilayer and the anion present in the solution affect the oxidation potential. The effect of the film thickness is small and, after the initial small increase, the potential stabilizes to a practically constant value (see Figure S1 in the Supporting Information). These changes probably reflect changes in the coordination

environment of the cerium ions in multilayers of different thickness and can be explained by the well-known three zone model of polyelectrolyte multilayers.²⁸ On the other hand, the anion effect is larger (see Table S1 in the Supporting Information). In acidic solutions, sulfate and perchlorate give the highest effective redox potential, but it drops considerably if chloride ions are present. This effect can be attributed to the complexation of cerium by chloride,²⁶ and complex formation with OH⁻ also explains the insensitivity of the redox potential to other ions in neutral solutions.

In our previous work, we have shown that these cerium-polyphosphate multilayers can be used for the electrodeless polymerization of pyrrole onto the film.⁷ The polypyrrole formation proceeds via initial oxidation of pyrrole monomers in the solution by the Ce(IV)/Ce(III) redox pair in the film. This process is clarified in a measurement of oxidation potential of a five bilayer film upon addition of monomeric pyrrole to an acidic (pH 1.5) solution upon stirring. The reaction is rapid and, within ca 30 minutes, the potential reaches a new plateau, which is approximately 580 mV lower than the initial potential (see Figure S2 in the Supporting Information). This means that the Ce(IV)/Ce(III) ratio in the films changes by more than ca 10 orders of magnitude during the process, i.e., practically all Ce(IV) will be consumed for the oxidation of the pyrrole monomers and the reaction stops after this reservoir of oxidant is used.

Thermodynamics sets the limits for the use of cerium-polyphosphate multilayers as oxidative films. Electrochemistry, and cyclic voltammetry especially, is an easy and controlled method to see whether certain molecules can be oxidized by the cerium-polyphosphate multilayer under given conditions. Figure 2 shows cyclic voltammograms of three conducting

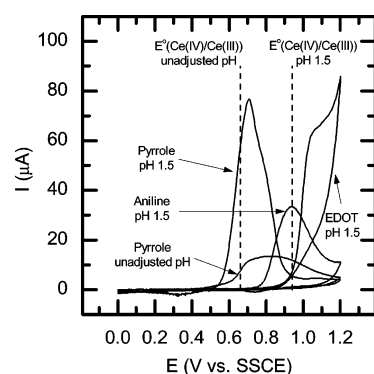


Figure 2. Cyclic voltammograms (on Au) in aqueous solutions containing 0.1 M Na₂SO₄ and pyrrole, EDOT or aniline. First voltammetric cycles in solutions containing 10 mM pyrrole (unadjusted pH and pH 1.5 adjusted with H₂SO₄), 10 mM EDOT (pH 1.5, adjusted with H₂SO₄), and 10 mM aniline (pH 1.5, adjusted with H₂SO₄).

polymer monomers, pyrrole, 3,4-ethylenedioxythiophene (EDOT), and aniline in aqueous solutions of pH 1.5. and for pyrrole, also in a near neutral solution with unadjusted pH. The extrapolation of the rising oxidizing current curve to zero current gives an estimate of the oxidation onset potential of the monomer in question. Also shown in the figure are the measured open-circuit potentials of a (PP/Ce)₅ multilayer under the same conditions (the film was aged for ca. 16 h). It is evident from the figure that the oxidation of pyrrole and aniline is thermodynamically highly favorable in acidic media and the

oxidation potential of the multilayer is sufficiently high for the oxidation of the EDOT monomer, too. The onset potentials for pyrrole, aniline and EDOT oxidation were +0.56, 0.78, and +0.93 V (vs SSCE), respectively, and the oxidation potential of the cerium-polyphosphate multilayer is +0.94 V. Although the onset potential of EDOT, determined from Figure 2, is very close to the redox potential of the film the voltammogram clearly shows that EDOT oxidation begins ca. 100 mV before the determined onset potential. However, the situation is different in unadjusted (~neutral) solutions, in which the film oxidation potential was only +0.60 V. This is only slightly more anodic than the pyrrole oxidation onset potential in these conditions, ca. +0.59 V, which is somewhat unambiguous, too, because of the form of the voltammogram in this case. Therefore, in acidic solution, the (PP/Ce)₅ multilayer provides a large enough thermodynamic driving force for reproducible oxidation of all tested monomers, while in the neutral solution the oxidation remains a borderline case. In addition, the polymerization mechanism is probably different in acidic and neutral conditions.^{21,29} In neutral solutions, acid-catalyzed polymerization of pyrrole results in nonconjugated dimer and trimer products and in the opening of the pyrrole ring with a concomitant nitrogen loss.³⁰ However, the formation of these solution-based products is slow and they give rise to only negligible contribution to the spectral changes observed upon the cerium-induced polymerization of pyrrole (see Figure S3 in the Supporting Information).

Formation of Conducting Polymer Films. In our earlier paper, we described the autopolymerization of pyrrole on thick Ce/PP multilayer films.⁷ However, although electroactive polypyrrole films could be obtained there were problems with the reproducibility, which can be traced to the use of neutral aqueous pyrrole solutions. In acidic solutions, the oxidation reaction is faster, which favors radical-radical coupling reactions, and the acidic milieu makes the reproducible polypyrrole film generation possible even with much thinner Ce/PP films than previously. In neutral solutions, the redox reaction is slow and the oligomeric species formed diffuse away from the surface without further coupling reactions (see Figure S4 in the Supporting Information).

On the other hand, when the PP/Ce multilayer is exposed to acidic (pH 1.5) pyrrole solution the formation of a polypyrrole film is clearly seen in the UV-vis spectra (Figure 3a). Concomitant to the reduction of cerium(IV) to cerium(III), visible at 290 nm, the formation of polypyrrole-based bands is evident above 400 nm. As discussed earlier, this reaction continues until all oxidant in the film is used. This conclusion is supported by the spectra of the multilayer before and after polypyrrole formation (Figure 3b), which shows that the band due to Ce(IV) at 290 nm is totally lost in the process. The spectrum of polypyrrole is dependent on its oxidation state but, according to the accepted bipolaron model, contains bands due to bipolarons (broad band at ca. 1200 nm), polarons (at 460–600 nm depending on the oxidation state) and the interband π – π^* transition below 400 nm.³¹ The difference spectra in Figure 3a show an increase in absorbance at 450 and at 800 nm. The former can be attributed to the small π – π^* transition observed at 450 nm in Figure 3b and the latter is part of the growing broad bipolaron band. Comparison of the absorbance values in Figure S3 in the Supporting Information and panels a and b in Figure 3 shows that the soluble acid-generated oligomers contribute very little to the observed spectrum at 450 nm. Similarly, the contribution of soluble, long oligomers to the

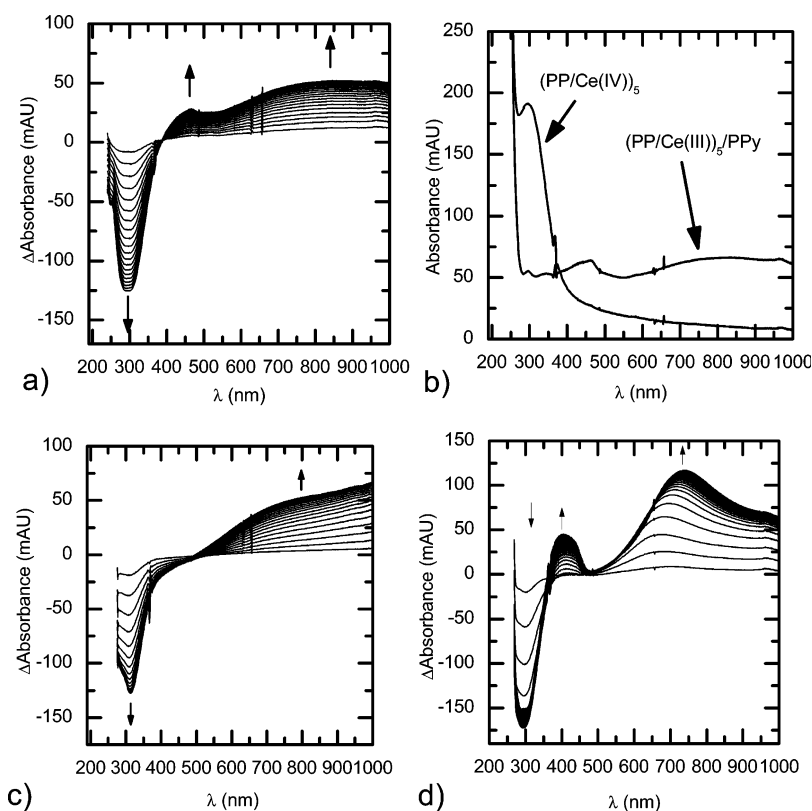


Figure 3. (a) UV-vis spectral changes during the reaction of $(\text{PP}/\text{Ce})_5$ film with 10 mM pyrrole in acidic solution (pH 1.5). (b) UV-vis spectrum of the multilayer film before and after exposure to pyrrole acidic conditions. (c) Spectral changes during the reaction of $(\text{PP}/\text{Ce})_5$ film with acidic (pH 1.5) 10 mM EDOT solution. (d) Spectral changes during the reaction of $(\text{PP}/\text{Ce})_5$ film with acidic (pH 1.5) 10 mM aniline solution. In a, c, and d, the spectra are taken at 4 min intervals and the spectrum of the $(\text{PP}/\text{Ce})_5$ film is taken as reference.

spectra recorded during the polymerization process is negligible, as shown by the similar shape and intensity of the band above 400 nm in spectra of the film during and after polymerization (Figure 3a, b). The polaron-induced band is usually rather weak but can be detected at ca 500 nm (and more clearly in the spectroelectrochemical measurements, *vide infra*). The effect of scattering is negligible and the spectra are characteristic of a conducting polypyrrole film at a moderately high oxidation state. Similarly, exposure to 10 mM EDOT solution in acidic conditions leads to the decrease of the Ce(IV) band and the increase of absorption above 500 nm, characteristic of the bipolaron-induced absorption bands in oxidized PEDOT polymer (Figure 3c), whereas in neutral solutions, the polymerization of EDOT does not proceed. We are aware of only one similar study, in which EDOT has been polymerized on templates (montmorillonite platelets) using cerium as a chemical oxidant.¹⁵ In addition, the same behavior is observed upon exposure of the film to a 10 mM acidic aniline solution. This leads to a clear decrease of cerium(IV) absorbance and to the simultaneous appearance of peaks characteristic to polyaniline (fig. 3d). All the oxidation tests show that PP/Ce multilayer film acts as a nonselective and universal oxidative surface. In acidic solution, the formation of a conducting polymer film on a PP/Ce multilayer takes place similarly as in electrochemical synthesis, i.e., via oxidative polymerization.

Film Characterization. In this work, we use polypyrrole as a model system for studying the autooxidative conducting polymer formation and film structure more closely. The morphology of the PP/Ce and $(\text{PP}/\text{Ce})_n/\text{PPy}$ films were

studied with AFM and SEM in order to gain more information about the film formation. The SEM images of the surface offer better resolution, showing a distribution of globular patterns with an average grain size of 30–50 nm (Figure 4b), similar to other studied polyphosphate-metal ion multilayer films.⁷ The AFM image of $(\text{PP}/\text{Ce})_5$ films exhibit a surface with spherical features (see Figure S5a in the Supporting Information) 50–100 nm in size and ca. 4 nm in height. Similar structures have been observed with polyphosphate-poly(allylamine hydrochloride) multilayer films, too, which suggests that the surface morphology can be largely attributed to polyphosphate.³² Both imaging techniques reveal that the oxidative cerium-polyphosphate multilayers have a highly granular structure, which strongly suggests that, during the layer-by-layer assembly, these films are formed by a nucleation and three dimensional growth mechanism.

The polymerization of pyrrole was allowed to go to the completion on thin ($n = 5$) and thick ($n = 15$) $(\text{PP}/\text{Ce})_n$ multilayers and the resulting films were imaged using both AFM and SEM (Figure 4b, c and Figure S5b, c in the Supporting Information). In both cases, irregular features attributed to polypyrrole form on the multilayer surface. The polypyrrole deposits are relatively thin, ca. 5 nm, and appear to form randomly on the underlying surface. With the thinner multilayer, polypyrrole does not fully cover the substrate, which is due to the limited amount of the oxidant, Ce(IV), available within a 5 bilayer film. However, the deposits formed are above the two-dimensional charge percolation threshold as shown by the electrical conductivity measurements (*vide infra*). On the thicker multilayer with a larger reservoir of the oxidant, the

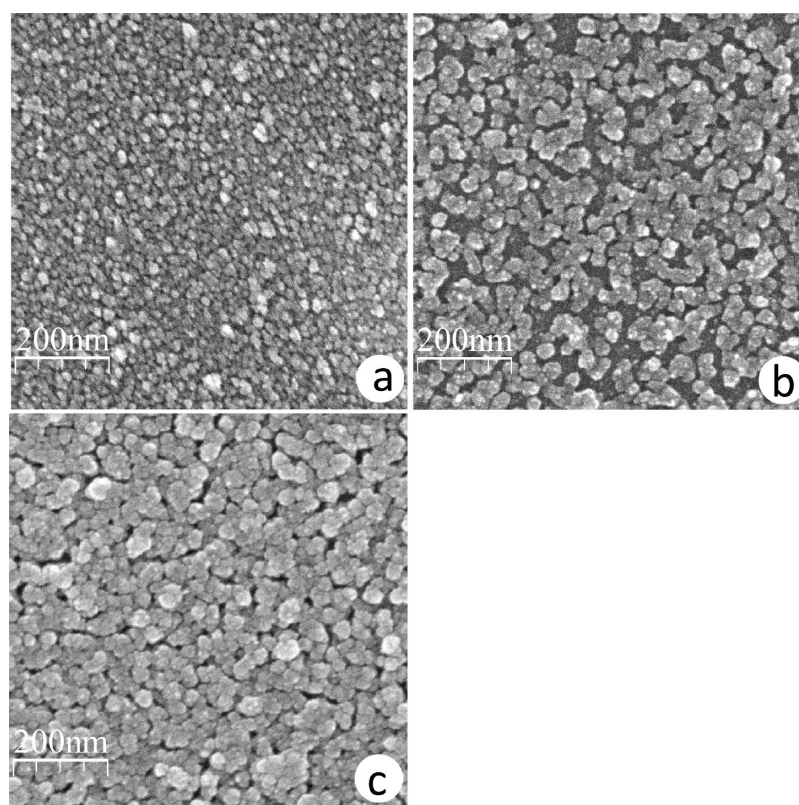


Figure 4. Scanning electron microscopy images of films. (a) $(\text{PP/Ce})_5$ multilayer film. (b) $(\text{PP/Ce})_5$ /polypyrrole film. (c) $(\text{PP/Ce})_{15}$ /polypyrrole film.

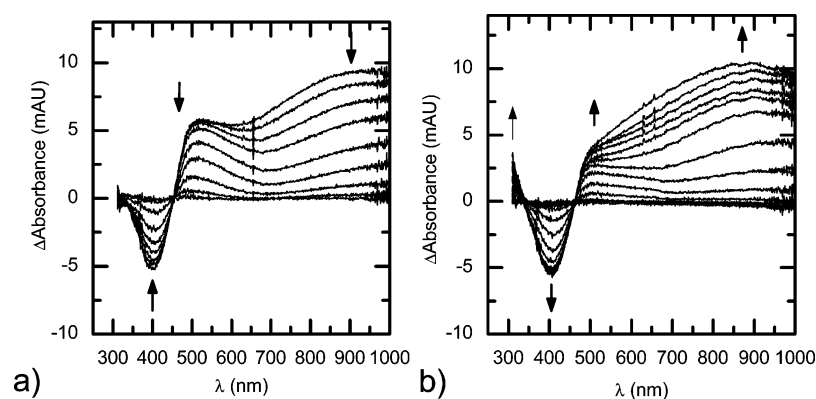


Figure 5. Difference spectra recorded during electrochemical (a) reduction and (b) oxidation of a $(\text{PP/Ce})_5$ /PPy film on glass/ITO electrode. The spectra are recorded in 0.1M Na_2SO_4 neutral water solution. Spectra taken from +0.06 V to -0.84 V vs. SSCE (reduction), and from -0.84 V to +0.46 V vs. SSCE (oxidation) at 0.1 V intervals (spectrum at -0.84 V is taken as reference).

polypyrrole deposits have grown together, mostly filling the open spaces between them. However, the average feature height is still relatively low, ca. 5 nm. This suggests that the polypyrrole film is formed on the PP/Ce multilayer by a nucleation and two-dimensional lateral growth mechanism. After polymerization, the sheet resistances and electrical conductivities of the films were $17.9 \text{ M}\Omega/\text{sq}$ (47 mS/cm) and $7.10 \text{ M}\Omega/\text{sq}$ (23 mS/cm) with the 5 bilayer (thickness 12 nm) and 15 bilayer (thickness 60 nm) PP/Ce multilayer films, respectively. The conductivities are clearly higher than reported for polypyrrole polymerized with cerium on montmorillonite platelets or fibrous phosphate films.^{14,16} In general, the conductivity of polypyrrole is highly dependent on the polymerization conditions and is usually in the range of 10

mS/cm to 300 S/cm .² In this work, the thickness of the polypyrrole film is of the order of only a few nanometers, and, especially with the thinner film, the film is not laterally uniform, either, indicating that the polypyrrole formed is well conducting. In materials coated with chemically polymerized polypyrrole, the measured conductivity can be higher but the polymer film is generally much thicker, too.²⁰ It should be noted that in our technique, too, the polymer loading can be increased by increasing the thickness of the oxidative multilayer, or by successively repeating the layer-by-layer and polymerization steps.⁷ The lower sheet resistance of the film on the thicker multilayer reflects the more uniform nature and higher connectivity of the polypyrrole layer compared to the polymer layer on the thin multilayer. However, the apparent

conductivity of the former is lower. The film thickness required for the calculation of the conductivity was obtained by AFM and corresponds to the total thickness of the film (PP/Ce multilayer and the polypyrrole layer). This suggests that the conducting layer is effectively formed only on the outer surface of the oxidative multilayer even though it partially interpenetrates through it and makes the film electroactive, as shown already in our previous work.⁷ The sheet resistances and apparent conductivities of PEDOT and polyaniline films formed on (PP/Ce)₅ multilayers are 580 MΩ/sq and 1 mS/cm, and 107 kΩ/sq and 4.2 S/cm, respectively. The rather large difference in the apparent conductivity can be enlightened by AFM images (see Figure S5 in the Supporting Information). Although the polyaniline film is extremely smooth and fully covers the substrate, the PEDOT film constitutes of isolated islands, probably not far above the percolation limit. The patchy distribution of PEDOT on the surface can be attributed to the low thermodynamic driving force and slow polymerization kinetics (vide infra). Although the formed polyaniline exhibits rather high conductivity, its stability is not as good as with polypyrrole. The green-colored polyaniline film detaches from the substrate under intense water rinsing, showing poorer anchoring of the polymer to the multilayer.

For a spectroelectrochemical characterization of polypyrrole films, we formed a (PP/Ce)₅/PPy film on a conducting ITO coated glass slide, which allows the adjustment of the redox state of the film by electrochemical means. Figure 5a shows the development of the polypyrrole spectrum when the film is reduced electrochemically from +0.06 V to -0.84 V vs. SSCE in neutral aqueous solution; reduction was started close to the rest potential of the film-coated electrode, +0.06 V. The displayed difference spectra are referenced to the spectrum at -0.84 V, which corresponds to neutral polypyrrole. During reduction, the absorbance due to the π - π^* transition at ca. 400 nm increases, whereas it decreases at wavelengths above 450 nm. However, the decrease does not take place evenly in this spectral region. Initial reduction is evident in the spectral region of the bipolaron band (above 700 nm) and, only later, in the range 450–600 nm characteristic of the polaron band (the initial increase of the interband transition is small and does not interfere with these observations). The two-stage redox process is even more clearly seen in the spectra taken during reoxidation of the film (Figure 5b). Initial oxidation is seen in the spectral range 450–700 nm, and the bipolaron band at lower energy starts to grow and dominate the spectrum only later. Comparison with the spectra recorded during the reduction shows the hysteresis of the redox process, characteristic to conducting polymers in general. It should be noted that the oxidation state of a pristine film is much lower than the maximum value electrochemically obtained (c.f. Figures 3 and 5), and it relaxes still further upon ageing, which is typical for electropolymerized conducting polymer films. In conclusion, the spectral changes are characteristic of conducting polypyrrole films and they show that cationic (polaron) and dicationic (bipolaron) species are involved in the redox processes of the film formed on oxidative PP/Ce multilayers.² Therefore, in a spectral and electrochemical sense, the polypyrrole film formed on oxidative PP/Ce multilayer is indistinguishable from electropolymerized films. In addition, concomitant to the decrease of the polypyrrole π - π^* -transition, an increase of absorbance below 350 nm can be seen during polypyrrole film reoxidation. This new band is attributed to the oxidation of Ce(III) to Ce(IV), which would

be seen at 290 nm, but the spectral window is limited due to the ITO glass substrate. Above pH 5 the oxidation potential of a Ce/PP multilayer is ca. +0.55 V vs SSCE (Figure 1b), which places the formal redox potential of the Ce(IV)/Ce(III) pair within the potential window used in the spectroelectrochemical measurements. Complexation of pyrrole by cerium may also change the redox properties of the metal but our previous XPS results gave no direct indication of pyrrole complexes in the film.⁷ This band was not detected during the reduction since the cerium inside the film was dominantly in the Ce(III) oxidation state after the polypyrrole film formation. The recharging of the Ce(IV) content within the film is especially noteworthy because the electrochemistry of bare PP/Ce multilayers is very sluggish. This suggests that polypyrrole acts as a kind of catalyst for the redox processes of cerium species in contact with it. In addition, the electroactivity of the polypyrrole film proves that the film partially penetrates through the Ce/PP multilayer to the ITO electrode surface as the sluggish cerium redox pair would not be able to mediate the necessary charge transfer.

All discussion of Ce/PP/PPy films has so far referred to results obtained using pyrrole concentration of 10 mM in the aqueous solution. In order to gain more insight into the factors affecting the film formation we have studied the effect of pyrrole concentration in acidic solution (pH 1.5). Three polypyrrole films were formed on (PP/Ce)₅ multilayers under otherwise identical conditions, and the reaction was allowed to proceed to completion in all cases (no spectral changes observed, see the Supporting Information, Figure S6), followed by rinsing of the cuvette to remove any soluble reaction products. Evidently, the higher the pyrrole concentration the more polypyrrole is formed but the yield of the product does not increase linearly with pyrrole concentration. The use of a 10 mM pyrrole solution results in only ca. 25% less polypyrrole than is obtained using a concentrated 100 mM pyrrole solution. In both cases the form of the spectrum is similar. When a very low concentration of pyrrole (1 mM) is used, the yield is ca. 20% of that obtained using a 10 mM pyrrole solution. However, even in this case, the spectral features are similar than seen in the two other cases, although much less pronounced. Although a more detailed discussion about the film formation process will be given below, the very low pyrrole concentration may cause the reduction of yield because the low concentration of initially formed small oligomers favor diffusion to the solution at the expense of film formation.

Polymerization Kinetics and Mechanism. The formation of a conducting polymer film on a Ce/PP multilayer is a complex and multiphase process. Here we divide it into two major parts in order to discuss the kinetics and mechanism of the process. The primary redox reaction, the initial reduction of Ce(IV), which signifies the oxidation of pyrrole monomers to radical cations, can be followed by the changes in the absorption band of Ce(IV) at 290 nm. The reaction pathway leading to the formation of polypyrrole is complex and not well-defined, including several coupling, deprotonation and oxidation reactions. Even the end product, the polypyrrole polymer, defies exact definition as a chemical species. Therefore, the study of the polymerization reaction itself is necessarily based on some approximations and can give only an average idea of the process. In this work, we have used the absorbance increase at 800 nm, which is within the bipolaron band of polypyrrole, as a measure of the extent of polypyrrole formation. A typical example of the evolution of absorbance at

these two wavelengths during the reaction of pyrrole on a (PP/Ce)₅ multilayer in acidic (pH 1.5) solution is shown in Figure 6. At both wavelengths, the reaction formally follows first-order

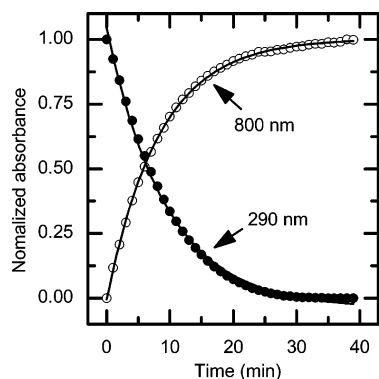


Figure 6. Changes in the normalized absorbance with time during the pyrrole polymerization reaction on a (PP/Ce)₅ multilayer film (10 mM pyrrole, pH 1.5). The process followed at two wavelengths, 290 and 800 nm (representing the primary redox reaction and the polymerization reaction, respectively). The solid lines show an exponential fit to the data.

kinetics (see Supporting Information, Figure S7). However, this is a heterogeneous reaction and the spectrally observed first-order behavior means that the areal concentrations of Ce(IV) and polypyrrole follow the equations

$$-\frac{d\Gamma(\text{Ce}^{\text{IV}})}{dt} = k_{\text{app},1}\Gamma(\text{Ce}^{\text{IV}})$$

$$\frac{d\Gamma(\text{PPy})}{dt} = k_{\text{app},2}\Gamma(\text{PPy})$$

where $\Gamma(\text{Ce}^{\text{IV}})$ and $\Gamma(\text{PPy})$ are the areal concentrations of Ce(IV) and polypyrrole, respectively, and $k_{\text{app},1}$ and $k_{\text{app},2}$ the corresponding apparent (pseudo-)first-order surface rate constants. The areal concentrations refer to an integrated amount of material in the path of the light beam of the spectrometer. The fact that the rate of reaction is always directly proportional to the areal concentration of Ce(IV) implies that diffusion of Ce(IV) within the film is not rate determining in the primary redox reaction. Our previous work on Ce/PP multilayers has shown that these multilayers resemble soft elastomers, which exhibit exponential layer-by-layer growth.⁷ This indicates that the cerium species are freely diffusing within the film. On the other hand, the direct proportionality of the rate of the polypyrrole film formation to the amount of the existing polypyrrole film suggests that the film formation reaction takes place effectively within the whole pre-existing polypyrrole film. Although cerium can diffuse freely within the multilayer, it may not be able to pass into the polypyrrole film. Rather, as the film is formed in the oxidized and conducting form, we envisage that electron transport between cerium in the multilayer and reacting pyrrole monomers takes place through the film to active locations in the growing polypyrrole film. One possibility is that the polypyrrole film is highly porous and all polymer material is accessible to pyrrole monomers. However, as the reaction proceeds, any existing pores should be filled, which would gradually decrease the observed rate of film formation. On the other hand, if the film formation takes place by nucleation and growth mechanism (Stranski–Kastranov) and the nuclei are

flat, effectively two-dimensional, the polypyrrole areal concentration will be proportional to the surface area of the growing nuclei before significant overlap of the nuclei. In fact, this latter suggestion is supported by the SEM and AFM images obtained at different stages of the film formation (vide supra).

To clarify the different stages of the complex reaction pathway we have studied the polypyrrole film formation using different solution concentration of pyrrole. As explained above, the yield of polypyrrole varies nonlinearly with the pyrrole concentration. On the other hand, in the concentration range 1–100 mM, both the primary redox reaction and the polymerization reaction exhibit pseudo first-order behavior (Table 1). If we express the observed rate constants in the form

$$k_{\text{app},1,2} = k_{1,2}[\text{py}]^\alpha$$

Table 1. Pseudo-First-Order Rate Constants Calculated from the Absorbance Changes at 290 and 800 nm

	$k_{\text{app},1}(290 \text{ nm})$ ($\times 10^{-4} \text{ s}^{-1}$)	$k_{\text{app},2}(800 \text{ nm})$ ($\times 10^{-4} \text{ s}^{-1}$)
pyrrole concentration (mM) ^a		
1	3.0	2.2
10	15.2	19.3
100	71.9	107
EDOT concentration (mM) ^b		
10	9.2	5.2
aniline concentration ^c		
10	17.1	10.0
number of bilayers ^d (absorbance at 300 nm)		
3 (0.10)	19.6	23.3
5 (0.23)	15.2	19.3
15 (1.27)	10.1	14.6

^aThe reactions were carried out on (PP/Ce)₅ multilayer film with different concentrations of pyrrole in pH 1.5. ^bThe reaction was carried out on (PP/Ce)₅ multilayer film with 10 mM EDOT in pH 1.5. ^cThe reaction was carried out on (PP/Ce)₅ multilayer film with 10 mM aniline in pH 1.5. ^dThe effect of layer thickness was studied with 10 mM pyrrole in pH 1.5

(where the rate constant $k_{1,2}$ still retains the dependence of the reaction rate on the cerium concentration) the primary redox reaction (followed at 290 nm) yields for the reaction rate constant $k_1(290 \text{ nm}) = (3.0 \pm 0.1) \times 10^{-4} \text{ M}^{-\alpha} \text{ s}^{-1}$ and for the order of the reaction with respect to pyrrole, $\alpha = 0.69 \pm 0.01$. This is very close to the theoretical value $\alpha = 2/3$, which would be expected if the reaction is first-order with respect to pyrrole and the diffusion of pyrrole to Ce(IV) at the surface is not rate-determining, as the pyrrole surface and bulk concentration are related by $[\text{py}]_{\text{surf}} = ([\text{py}]_{\text{bulk}})^{2/3}$. On the other hand, the polymerization reaction yield much poorer dependence on the pyrrole concentration ($k_2(800 \text{ nm}) = (2.4 \pm 0.5) \times 10^{-4} \text{ M}^{-\alpha} \text{ s}^{-1}$, $\alpha = 0.84 \pm 0.06$) and the apparent reaction order decreases with pyrrole concentration. The rate of the polymerization increases more rapidly than the reduction rate of Ce(IV), which shows that the polymerization reaction is a nonlinear process with respect to pyrrole concentration. The complexity of the process hampers its more detailed analysis but the acceleration of the polymerization may be attributed to various coupling reactions between oligomeric species and oligomers and (oxidized) monomers required for the film formation.

The study of the effect of cerium on the kinetics of the film formation process is not straightforward because we cannot

control the loading of cerium in the multilayer. However, we can control the total amount of oxidant by the number of the Ce/PP bilayers, which can be quantitated by the absorbance at the Ce(IV) band. The addition of more bilayers also increases the thickness of the oxidative multilayer and, therefore, yields some idea about the effect of charge transfer and oxidant accessibility in the multilayer. The measurements with different number of bilayers showed that the reaction rates are affected by the multilayer thickness but the reactions always follow the pseudo first-order kinetics (Table 1). The rates of both the primary redox reaction and the polymerization reaction decrease with increasing multilayer thickness. However, in the studied thickness range (3–15 bilayers) the changes were small, amounting only to a 40–50% decrease in the apparent rate constants. Interestingly, the primary redox reaction was slowed down more than the subsequent polymerization. On the basis of the previous discussion, the diffusion of charge or pyrrole is not assumed to be rate limiting even with thick multilayers. Instead, the dependence of the reaction rates on the number of PP/Ce bilayers implies that the effect is connected to the variation of the multilayer properties. In fact, the required dependence of the properties and structure of the multilayer is suggested by the well-known three zone model.²⁸ As the formation of a multilayer begins the first layers constitute zone I, which is strongly influenced by the substrate surface. When the number of layers is increased, the solution-film interface, zone III, is then formed, followed by the creation of zone II representing the multilayer bulk. Zone I is generally rather compressed and the highly solvated zone III quite diffuse, the bulk phase (zone II) being somewhere in between these interfacial regions of the film. Therefore, the concentration of cerium within the multilayer may be dependent on position. In fact, comparison of the cerium absorbance (proportional to the amount of cerium in the film) and the total mass of the PP/Ce multilayer, determined by quartz crystal impedance and taken as a qualitative indicator of the film volume, suggests that the effective cerium concentration decreases as the number of PP/Ce bilayers increases (Figure 7). We must emphasize that we

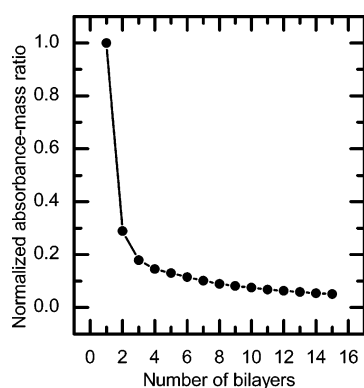


Figure 7. Absorbance-mass ratio of PP/Ce multilayer. The normalized ratio is calculated by dividing the film absorbance at 290 nm by the mass of the film obtained by QCM.

cannot measure the exact variation of the cerium concentration as a function of film thickness because the measured film mass also includes water trapped in the film. However, the observed behavior of the absorbance/mass ratio leads us to attribute the trend in the reaction rate to the decreased effective oxidant concentration in thicker multilayers. The increase in the relative

rate of the polymerization with respect to the primary redox reaction is similar as observed above in the study of the effect of pyrrole concentration, and can be attributed to similar factors. On the other hand, the oxidative capacity increases with the multilayer thickness, yielding larger amounts of polypyrrole. The amount of produced polypyrrole is linearly proportional to the initial amount of Ce(IV) in the film, which is in accordance with the observed exhausting of all Ce(IV) oxidant during the reaction. The result also shows that the amount and thickness of the conducting polymer can be controlled simply by the number of oxidative layers.

Similar first-order kinetics was observed for both principal reactions also when EDOT or aniline was used. For the EDOT monomer, the apparent rate constants for the primary and polymerization reaction are clearly lower than the corresponding values for pyrrole. This reflects the smaller thermodynamic driving force in the case of EDOT and, for the polymerization reaction, also the greater tendency of the monomer radical cations to get consumed in unwanted side reactions. For aniline, the oxidation onset potential (Figure 2) under the experimental conditions is so much below the formal redox potential of the PP/Ce multilayer that the rate of the primary redox reaction is practically the same as with pyrrole. On the other hand, the rate of the polymer formation, which depends on the pathway of the polymerization reaction of each monomer, is between that of EDOT and pyrrole. In all cases, however, the film formation is fast enough for practical applications, and a conducting film can be formed in the time scale of 30–60 min.

CONCLUSIONS

We have shown that thin layer-by-layer deposited cerium polyphosphate multilayers provide a general template for the electrodeless oxidative polymerization of various conducting polymers from aqueous solution. The effective oxidation potential of the Ce/PP multilayers depends on the solution pH, ions in solution, age of the film and the number of layers. However, the multilayers are effective oxidants and we have demonstrated that they can polymerize, e.g., pyrrole, aniline and 3,4-ethylenedioxythiophene, and form thin well-conducting polymer layers in a time scale of ca 30 minutes. The conducting polymer films formed are spectrally and electrochemically indistinguishable from conventional electropolymerized films.

In this work, we have confirmed that acidic conditions are optimal for the polymerization reaction. The rate of polymer formation and the thickness of the conducting film can be controlled by the concentration of the monomer in solution and the number of cerium/polyphosphate bilayers in the oxidative film. Kinetic studies show that the film formation is not restricted by charge diffusion in the film and follows apparent first-order kinetics. The polymer film forms via a nucleation and two-dimensional growth mechanism on the outer layer of the oxidative film and the reaction proceeds until all oxidant, i.e., Ce(IV), within the multilayer is consumed. However, it also partially extends through the underlying multilayer, making the film electroactive, which enables the electric control of the properties of the polymer film. The conducting polymer film also facilitates the redox reactions of the otherwise sluggish Ce(IV)/Ce(III) pair in the multilayer.

The layer-by-layer film technique is insensitive to the size, shape or chemical nature of the substrate surface. Therefore, these oxidative Ce/PP multilayers enable a facile formation of thin conducting polymer films on a large variety of substrates.

The formation of both the oxidative multilayer and the conducting polymer film requires only the exposition of the substrate to dilute aqueous solutions of the components (cerium(IV) and polyphosphate, and the appropriate monomer, respectively), e.g., by a simple dipping technique, and can be easily applied to numerous applications under ambient conditions without any expensive and complicated instrumentation or strict environmental control. In addition, our recent work shows that the technique is not limited to the materials discussed here but both the metal and the polyanion can be exchanged, e.g., the former to Fe(III) and the latter to poly(acrylic acid) or some other carboxylate-based polyanion.

■ ASSOCIATED CONTENT

■ Supporting Information

Oxidation potential of PP/Ce multilayers as a function of layers; Effect of anions on the oxidation potential of the film; Effect of pyrrole addition on the oxidation potential; Effect of pyrrole in the presence of a redox inactive (PP/Zr)₅ multilayer; Spectral changes during the reaction of (PP/Ce)₅ film with pyrrole in a neutral solution; AFM figures of PP/Ce multilayers with conducting polymers; Logarithmic representation of absorbance in 800 nm vs. time consumed for polymerization reaction; Spectra of polypyrrole formed on (PP/Ce)₅ films in different pyrrole concentrations. This material is available free of charge via the Internet at <http://pubs.acs.org/>.

■ AUTHOR INFORMATION

Corresponding Author

*E-mail: mikko.salomaki@utu.fi.

Notes

The authors declare no competing financial interest.

■ ACKNOWLEDGMENTS

Grants 139624 and 128535 from the Academy of Finland are gratefully acknowledged.

■ REFERENCES

- (1) Decher, G. *Science* **1997**, *277*, 1232–1237.
- (2) Skotheim, T.; Reynolds, J.; Elsembamer, R., Eds.; In *Handbook of Conducting Polymers*, 2nd ed.; Marcel Dekker: New York, 1998.
- (3) Cheung, J.; Fou, A.; Rubner, M. *Thin Solid Films* **1994**, *244*, 985–989.
- (4) Ferreira, M.; Rubner, M. *Macromolecules* **1995**, *28*, 7107–7114.
- (5) Lukkari, J.; Salomaki, M.; Viinikanoja, A.; Aaritalo, T.; Paukkunen, J.; Kocharova, N.; Kankare, J. *J. Am. Chem. Soc.* **2001**, *123*, 6083–6091.
- (6) DeLongchamp, D.; Hammond, P. T. *Adv. Mater.* **2001**, *13*, 1455–1459.
- (7) Salomaki, M.; Rasanen, M.; Leiro, J.; Huti, T.; Tenho, M.; Lukkari, J.; Kankare, J. *Adv. Funct. Mater.* **2010**, *20*, 2140–2147.
- (8) Nair, V.; Deepthi, A. *Chem. Rev.* **2007**, *107*, 1862–1891.
- (9) Sarac, A.; Erbil, C.; Ustamehmeoglu, B. *Polym. Bull.* **1994**, *33*, 535–540.
- (10) Sarac, A.; Ustamehmeoglu, B.; Mustafaev, M.; Erbil, C.; Uzelli, G. *J. Polym. Sci., Polym. Chem.* **1995**, *33*, 1581–1587.
- (11) Saraç, A. S.; Erbil, C.; Soydan, A. B. *J Appl Polym Sci* **1992**, *44*, 877–881.
- (12) Erbil, C.; Cin, C.; Soydan, A. B.; Sarac, A. S. *J Appl Polym Sci* **1993**, *47*, 1643–1648.
- (13) Erbil, C.; Ustamehmeoglu, B.; Uzelli, G.; Sarac, A. *Eur. Polym. J.* **1994**, *30*, 149–152.
- (14) Verissimo, C.; Alves, O. *J. Mater. Chem.* **2003**, *13*, 1378–1383.

- (15) Rajapakse, R. M. G.; Higgins, S.; Velauthamurty, K.; Bandara, H. M. N.; Wijeratne, S.; Rajapakse, R. M. M. Y. *J. Composite Mater.* **2011**, *45*, 597–608.
- (16) Rajapakse, R. M. G.; Murakami, K.; Bandara, H. M. N.; Rajapakse, R. M. M. Y.; Velauthamurty, K.; Wijeratne, S. *Electrochim. Acta* **2010**, *55*, 2490–2497.
- (17) Partch, R.; Gangolli, S.; Matijevec, E.; Cai, W.; Araj, S. *J. Colloid Interface Sci.* **1991**, *144*, 27–35.
- (18) Galebeck, A.; Alves, O. *Synth. Met.* **1997**, *84*, 151–152.
- (19) Galebeck, A.; Alves, O. *Synth. Met.* **1999**, *102*, 1238–1239.
- (20) Omastova, M.; Micusik, M. *Chem. Pap.* **2012**, *66*, 392–414.
- (21) Sadki, S.; Schottland, P.; Brodie, N.; Sabouraud, G. *Chem. Soc. Rev.* **2000**, *29*, 283–293.
- (22) Kankare, J.; Loilkas, K.; Salomaki, M. *Anal. Chem.* **2006**, *78*, 1875–1882.
- (23) Salomaki, M.; Kankare, J. *J Phys Chem B* **2007**, *111*, 8509–8519.
- (24) Bishop, E.; Cofre, P. *Analyst* **1981**, *106*, 316–322.
- (25) Zingales, R. *J. Chem. Soc., Dalton Trans.* **1990**, 229–234.
- (26) Maverick, A.; Yao, Q. *Inorg. Chem.* **1993**, *32*, 5626–5628.
- (27) Schweitzer, G. K.; Pesterfield, L. L. In *The Aqueous Chemistry of the Elements*; Oxford University Press: Oxford, U.K., 2010; .
- (28) Ladam, G.; Schaad, P.; Voegel, J. C.; Schaaf, P.; Decher, G.; Cuisinier, F. *Langmuir* **2000**, *16*, 1249–1255.
- (29) Qian, R.; Pei, Q.; Huang, Z. *Macromol. Chem. Phys.* **1991**, *192*, 1263–1273.
- (30) Hawkins, S.; Ratcliffe, N. *J. Mater. Chem.* **2000**, *10*, 2057–2062.
- (31) Bredas, J.; Street, G. *Acc. Chem. Res.* **1985**, *18*, 309–315.
- (32) Cini, N.; Tulun, T.; Decher, G.; Ball, V. *J. Am. Chem. Soc.* **2010**, *132*, 8264–8265.